

Codebook Configuration for 1-bit RIS-aided Systems Based on Implicit Neural Representations

Yao Xiao^{*}, Zhijie Fan^{*}, Zenan Ling[†], Rujing Xiong, Tiebin Mi, Robert Caiming Qiu
EIC, Huazhong University of Science and Technology, Wuhan 430074, China.
^{*} Equal contribution. [†] Corresponding Author. Email: lingzenan@hust.edu.cn

Abstract—Reconfigurable intelligent surfaces (RISs) have become one of the key technologies in 6G wireless communications. By configuring the reflection beamforming codebooks, RIS focuses signals on target receivers. In this paper, we investigate the codebook configuration for 1-bit RIS-aided systems. We propose a novel learning-based method built upon the advanced methodology of implicit neural representations. The proposed model learns a continuous and differentiable coordinate-to-codebook representation from samplings. Our method only requires the information of the user’s coordinate and avoids the assumption of channel models. Moreover, we propose an encoding-decoding strategy to reduce the dimension of codebooks, and thus improve the learning efficiency of the proposed method. Experimental results on simulation and measured data demonstrated the remarkable advantages of the proposed method.

Index Terms—RIS, codebook, learning-based method, implicit neural representation.

I. INTRODUCTION

Reconfigurable intelligent surfaces (RISs) have recently emerged as a promising technology to extend the wireless network’s coverage and improve the transmission quality [1]–[3]. By careful configuration of the corresponding reflection beamforming *codebooks*, RISs reflect signals and focus them on the target receivers. Theoretically, the elements of RISs are considered to be continuous, meaning that they can continuously adjust the amplitude and the phase of incident radio waves. But in practice, the properties of radio waves always be discretely changed by the elements of RISs. Therefore, in this paper, we focus on the codebook configuration for 1-bit RISs whose elements have two possible configurations.

A large body of work has been devoted to the study of the codebook configuration for 1-bit RISs. On one hand, many previous works are model-based. Some approaches [1], [4]–[7] address the related continuous problems first, and then solve 1-bit codebooks by discreteization. Alternatively, [8]–[12] develop discrete optimization algorithms, e.g., heuristic alternating optimization, to directly solve discrete codebooks. However, model-based methods face difficulties in practical scenarios due to the simplification and assumption of channel models, the requirement of extra source device information, and the complexity of the optimization. On the other hand, learning-based approaches learn the configuration of codebooks from the collected data. [13] apply reinforcement learning algorithms to configure codebooks depending on feedback from receivers’ feedback, e.g., received signal strength or received signal-to-noise ratio. However, these methods require

the real-time feedback which is hard to achieve in practice. Moreover, [14] proposes a vanilla multilayer perceptron (MLP) on simulation data to learn a map from 2D coordinates to codebooks. However, due to the limited expressivity of vanilla MLPs, this approach is difficult to apply to complex scenarios in practice.

In this paper, we formulate the 1-bit RISs codebook configuration as a multi-label classification problem [15], and propose a novel learning-based approach based on *implicit neural representations* (INR) [16], [17]. Given users’ 3D coordinates, the proposed model is trained on the collected data to learn the corresponding codebooks of 1-bit RISs. During deployment, the learned model can accurately configure codebooks only using users’ 3D coordinates. The proposed approach avoids model dependency, does not require extra source information, and has a relatively low time overhead, making it straightforward to deploy in practical scenarios.

Solving such a learning problem is challenging due to the limited information in coordinates, the discrete nature of the label, and the complicated correlations between coordinates and the corresponding codebooks. INRs appear very natural for the problem at hand. INR is a continuous and differentiable representation, which enables the effective gradient-based training, but has remarkable advantages in a wide variety of tasks of modeling discrete signals, e.g., the image restoration and the novel view synthesis (NVS) [18], [19]. For the first time, we introduce the INR technique to the wireless communication community, and show its significant advantage in 1-bit RIS codebook configuration.

Furthermore, we develop an encoding method to compress codebooks. INR needs to predict $M \times N$ labels for a 1-bit RIS of size $M \times N$. This implies that INR needs to learn an extremely large state space with the increase of M, N . It will decrease the training efficiency and increase the risk of over-fitting. To mitigate this problem, we develop an encoding method to reduce the length of each label vector to be only $M+N-1$. A corresponding decoding method is also designed to restore predicted results back to original codebooks. As such, the encoding method is *lossless*.

Our contributions are summarized as follows.

- We propose a novel INR method to configure codebooks of 1-bit RISs. From discrete sampling, our method learns a continuous and differentiable coordinate-to-codebook representation. To the best of our knowledge, this is the first time INRs have been applied to this problem.

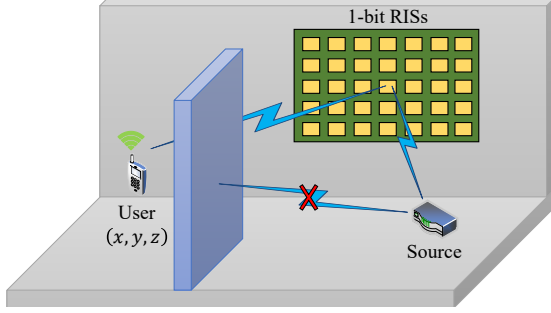


Fig. 1. The considered 1-bit RISs-assisted communication system. Our goal is to configure the 1-bit optimal codebook only using user coordinates.

- We propose a lossless encoding and decoding approach to reduce the dimension of the state space of 1-bit RIS codebooks. The proposed approach benefits the training and the generalization of INRs.
- We conduct experiments on both simulation and measured datasets. Experimental results demonstrate the dramatic advantage of our method.

II. PROPOSED METHODOLOGY

In this study, we investigate a practical scenario of a 1-bit RISs-aided wireless communication system, illustrated in Fig. 1. We assume a fixed configuration for both the 1-bit RISs and the signal source. The 1-bit RISs consist of M rows and N columns of elements, where each element's configuration is represented by a logic value of "1" or "0", forming an $M \times N$ -dimensional boolean matrix, denoted as the codebook. In this scenario, users behind obstacles experience inadequate signal strength through the line-of-sight link. To address this issue, it is necessary to configure an optimal codebook, that enables 1-bit RISs to converge reflected radio waves towards users and enhance the received signal strength. Consequently, the problem at hand becomes determining the optimal codebook for maximizing signal strength at any user's location, which is described as:

$$\Phi_{\mathbf{p}}^* = \arg \max_{\Phi_{\mathbf{p}}} E(\Phi_{\mathbf{p}}), \quad s.t. \quad \Phi_{\mathbf{p}} = \{0, 1\}^{M \times N}, \quad (1)$$

where $\mathbf{p} := (x, y, z)$ represents the coordinates of the user, $\Phi_{\mathbf{p}}$ denotes the codebook configuration of 1-bit RISs and E represents the received signal strength of the user. The objective in this paper is to configure the optimal codebook $\Phi_{\mathbf{p}}^*$ for the user at any location \mathbf{p} to maximize the received signal strength.

Numerous works have proposed solutions to solve (1). However, existing model-based approaches heavily rely on the construction of accurate channel models, which often make assumptions and relaxations that are challenging to satisfy in practical scenarios. Additionally, certain feedback-based methods require users to provide real-time optimization metrics and involve relatively high time overhead which are also challenging to meet in practical scenarios. These

shortcomings motivate us to design an efficient data-driven codebook configuration method for 1-bit RISs.

A. Implicit Neural Representation

In this paper, our goal is to learn a mapping function from user's coordinates to the corresponding optimal 1-bit codebook. Recently, INR has been proposed as a powerful tool for tasks of mapping coordinates to desired outputs, e.g. the NVS task. As shown in Fig. 2(b), we observe the similarity between the problem at hand and the NVS task. Inspired by such similarity, we propose to utilize INRs to learn the mapping relationship from user coordinates to the optimal 1-bit codebooks. Specifically, the proposed INR model consists of two main components: an unlearnable positional encoding (PE) mapping function and a learnable MLP, as shown in Fig. 2(a).

1) *Positional Encoding*: The PE function $\gamma(\cdot)$ based on Fourier transform can map the normalised user coordinates to a high-dimensional space. Specifically, PE function takes the normalised user coordinates $\mathbf{p}' := (x', y', z')$ as the input, and performs an upscaling mapping on each dimension as

$$\gamma(\mathbf{p}') = \begin{bmatrix} \sin(b^0 \pi \mathbf{p}'), \cos(b^0 \pi \mathbf{p}'), \\ \dots, \\ \sin(b^{L-1} \pi \mathbf{p}'), \cos(b^{L-1} \pi \mathbf{p}') \end{bmatrix}, \quad (2)$$

where b is the base frequency, and L is the dimension of mapping space. Consequently, the input dimension of the MLP is transformed from 3 to $6L$.

2) *Multi-Layer Perceptron*: The MLP architecture we designed to learn the mapping relationship from user coordinates to the optimal 1-bit codebooks is shown in Fig.4(a). It consists of five layers: the input layer, three hidden layers, and the output layer. The number of perceptrons in the input layer, three hidden layers, and output layer are $6L$, 64, 64, 64, and $M + N - 1$, respectively. The three hidden layers utilize the $ReLU(\cdot)$ activation function to learn the mapping relationship from user coordinates to the 1-bit optimal codebooks. The output layer employs the $sigmoid(\cdot)$ activation function and is coupled with the binary cross-entropy (BCE) [20] loss function for backpropagation and parameter updates, since we are essentially solving a multi-label classification problem.

B. Encoding and Decoding Scheme

For optimal 1-bit codebooks obtained by the row-column traversal algorithm, we design an encoding method. As shown in Fig. 3(a), the proposed encoding method can use only $M + N - 1$ binary variables to uniquely represent 1-bit codebooks of size $M \times N$. Moreover, the proposed encoding method is *lossless*, which means that the original codebook can be recovered from encoded results through a corresponding decoding method as shown in Fig. 3(b). With this encoding-decoding method, we only need to predict $M + N - 1$ labels, and then decode the predicted results to configure the 1-bit optimal codebooks, which mitigates the challenges arising from the high-dimension of the output layers.

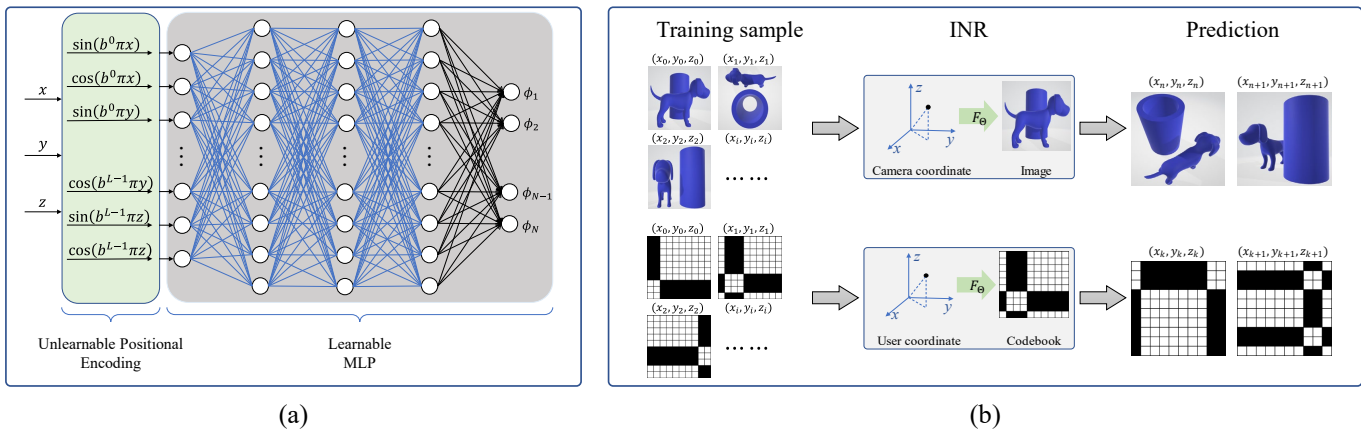


Fig. 2. (a) The architecture of INRs. (b) Similarity between the NVS task and the code book configuration for 1-bit RISs.

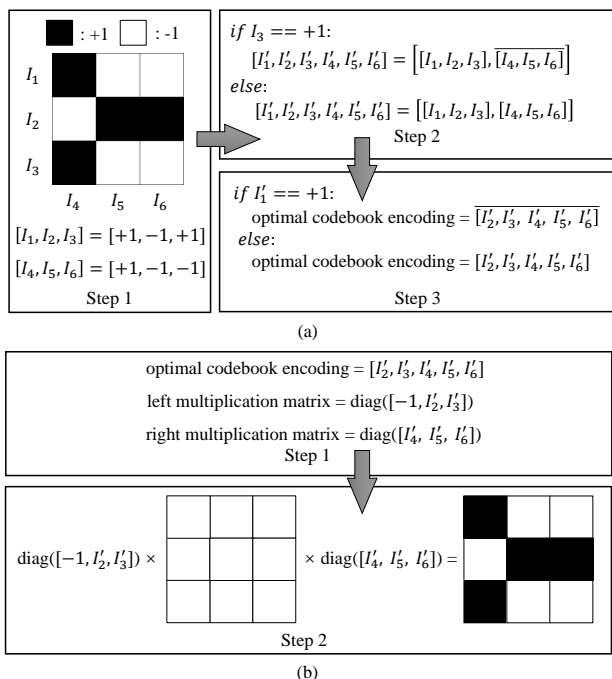


Fig. 3. The designed encoding and decoding scheme, taking 3×3 1-bit RISs as an example. To ensure the accuracy of the expression, only in this figure, we use “+1” and “-1”, instead of “1” and “0” to represent the configuration of elements. (a) The designed lossless encoding scheme, uses $M + N - 1$ binary variables to uniquely represent the $M \times N$ 1-bit optimal codebooks obtained through the row-column traversal algorithm. (b) The decoding scheme, enables the restoration of the encoded results to the configuration of the 1-bit optimal codebooks.

III. MODEL TRAINING AND DEPLOYMENT

A. Dataset Construction

To construct the training dataset, We uniformly set K sampling points $\mathbf{p}_1, \mathbf{p}_2, \dots, \mathbf{p}_K$ in the space where users may appear, and search for the optimal 1-bit codebook for each sampling point using a traversal algorithm.

In order to obtain stable and high-performance results at a fast speed, we adopt an alternative approach called row-column traversal algorithm. The algorithm starts with an all

“0” codebook, inverts the configuration of all components on each row and column in turn, and calculates the received signal strength after each inverse. If the inverse leads to an improvement in the received signal strength, the algorithm keeps it; otherwise, reverts it. This process is repeated until the codebook no longer changes, indicating that the algorithm has reached the final result. Extensive experimental results have shown that the row-column traversal algorithm has relatively fast speed, stable results, and performance close to the theoretical optimum. We use the row-column traversal algorithm to obtain the optimal 1-bit codebook as the label and construct the dataset D :

$$D = \{(\mathbf{p}_1, \Phi_{\mathbf{p}_1}^*), (\mathbf{p}_2, \Phi_{\mathbf{p}_2}^*), \dots, (\mathbf{p}_K, \Phi_{\mathbf{p}_K}^*)\} \quad (3)$$

B. Training and Deployment

Our framework is illustrated in Fig. 4, which consists of two parts: the training phase and the deployment phase.

1) *Training Phase*: We denote the INR model as $f_\theta(\mathbf{p}) = \mathbf{h}$, where θ is the trainable parameters, \mathbf{p} is the user’s coordinate, and \mathbf{h} is the multi-label vector with a length of $M + N - 1$ predicted by INR model. The training phase is formulated as,

$$\arg \min_{\theta} \ell(f_\theta(\mathbf{p}) - \text{encoder}(\Phi_{\mathbf{p}}^*)) \quad (4)$$

where $\Phi_{\mathbf{p}}^*$ is the ground-truth codebook for user at the coordinate \mathbf{p} , and encoder is the lossless encoding scheme that can encode the $M \times N$ -dimensional $\Phi_{\mathbf{p}}^*$ into a binary vector of length $M + N - 1$. In the training phase, we want the output \mathbf{h} of the INR model to fit the optimal 1-bit codebook encoding result $\text{encoder}(\Phi_{\mathbf{p}}^*)$ by updating the weights θ .

2) *Deployment Phase*: Given a learned INR model f_θ , we formulate the deployment phase as,

$$\mathbf{h}_{\text{real}} = f_\theta(\mathbf{p}_{\text{real}}), \quad \mathbf{H}_{\text{real}} = \sigma(\mathbf{h}_{\text{real}}), \\ \hat{\Phi}_{\mathbf{p}} = \text{decoder}(\mathbf{H}_{\text{real}})$$

where \mathbf{p}_{real} is the coordinate of the real user, \mathbf{h}_{real} is the predicted output of trained INR model, function $\sigma(\cdot)$ maps the input in the range of 0 to 0.5 to 0, and maps the input

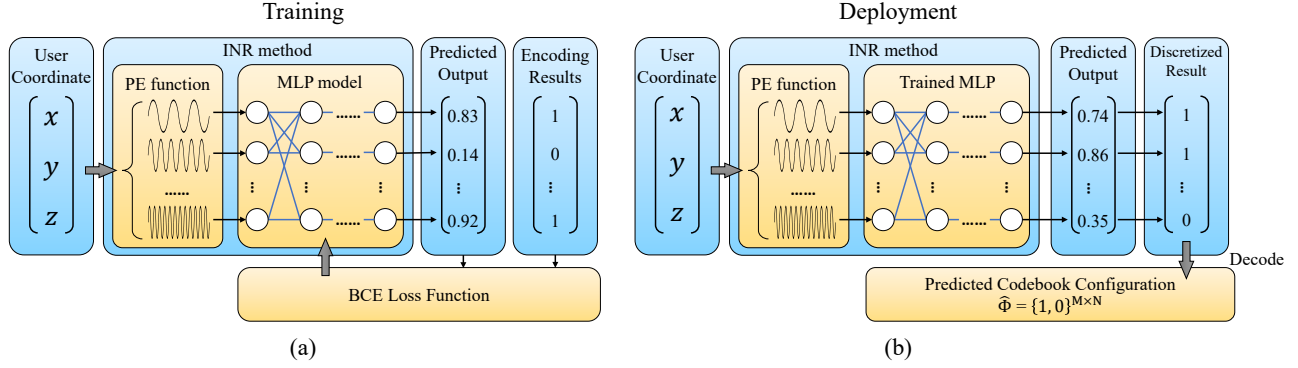


Fig. 4. Our framework is divided into two parts: the training phase and the deployment phase. During the training phase, the INR model is trained on the (user coordinate, encoded 1-bit optimal codebook) dataset. During the deployment, the model can configure the optimal codebook only using the user coordinate.

in the range of 0.5 to 1 to 1, $\text{decoder}(\cdot)$ is the corresponding decoding scheme which can restore \mathbf{H}_{real} to the $M \times N$ dimensional 1-bit codebook $\hat{\Phi}_{\text{p}}$.

IV. EXPERIMENT

We conduct experiments on both simulated and measured data to evaluate the proposed INR-based method in a Single-Input Single-Output RIS-system. The key parameters in the experiments of the proposed method are summarized in Table I. Specifically, we constructed a simulation environment and an experimental environment, and built the optimal codebook dataset through search algorithm. Four benchmarks are adopted for comparison:

- **vanilla MLP**: Basic MLP neural network [14].
- **APX**: Approximation algorithm [21].
- **SDR**: Semi-definite relaxation [22].
- **Maniopt**: Manifold optimization [23].

A. Dataset Construction and Evaluation Metrics

1) *Simulation Dataset*: We construct a simulation environment as shown in Fig. 5(a), where the user and the signal source are distributed on both sides of the obstacle. The user cannot receive the signal from the source except through the 10×10 1-bit RISs deployed on the wall. We define a three-dimensional space where the user will be positioned with dimensions of 2 meters in length, width, and height. And $21 \times 21 \times 21 = 9,261$ sample points are set up, with a spacing of 0.1 meters between adjacent sample points. Based on [24], [25], we model a 1-bit RIS-assisted system from an electromagnetic field perspective. This model can calculate the signal strength at any point in space depending on the current codebooks. Consequently, we utilize the proposed row-column traversal algorithm to obtain the optimal codebook for each sampling point and construct the simulation dataset.

2) *Measured Dataset*: We constructed an experimental scenario as shown in Fig. 5(b). It includes a USRP device for generating modulated signals and demodulating received signals. Two horn antennas, which are capable of transmitting or receiving signals in specific directions, are used to simulate the situation where the line-of-sight link is obstructed. The

10×16 1-bit RISs are utilized to assist the communication between the transmitter and receiver. And the mobile platform provides an accessible space of $1m \times 0.7m \times 2m$, allowing precise movement of the receiver. We set up $15 \times 21 \times 41 = 12,915$ sampling points with a spacing of 0.05 meters between adjacent points. Based on the received signal strength at the receiver, we employ the row-column traversal algorithm to obtain the optimal codebook for each sampling point, thereby constructing the measured dataset.

3) *Evaluation Metrics*: The evaluation metrics used are the average accuracy of reflector unit phase and the received signal strength at the receiver. The unit phase accuracy of reflector unit is defined as:

$$\text{Accuracy} = \frac{\text{number of correct predictions}}{\text{total number of predictions}}.$$

Received signal strength is measured by power. We deploy the codebooks obtained by different methods in the RIS system and measure the received signal strength at the receiver.

B. Training and Experimentation

1) *Data Processing*: Prior to MLP training, dataset D undergoes data processing. The coordinates data are scaled to the range of $[-1, +1]$, transformed into a $6L$ dimensional vector using the PE function $\gamma(\cdot)$, which serves as the MLP input. And the encoding scheme $g(\cdot)$ is utilized to encode the 1-bit optimal codebooks in D , producing binary vectors of length $M + N - 1$ as the labels for MLP training.

2) *MLP Training*: During training, we use the $6L$ dimensional vectors as the MLP input and the $M + N - 1$ dimensional binary vectors $g(\Phi)$ as the labels. We use the BCE loss function to measure the difference between $g(\Phi)$ and MLP output \mathbf{h} , training the MLP weights θ :

$$\ell(g(\Phi), \mathbf{h}) = - \sum_{i=1}^{M+N-1} [g_i \log(h_i) + (1 - g_i) \log(1 - h_i)]$$

where g_i represents the i -th element of $g(\Phi)$ and h_i represents the i -th element of \mathbf{h} . We use stochastic gradient descent (SGD) algorithm to update the MLP parameters,

$$\theta_{t+1} = \theta_t - \eta \nabla \ell(\theta_t)$$

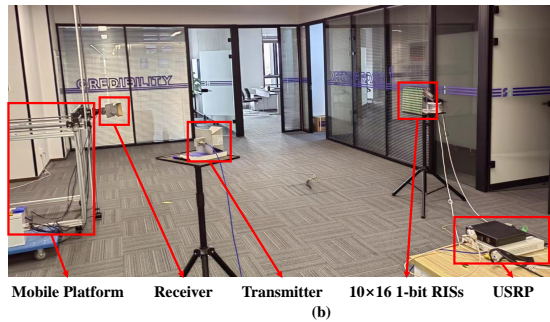
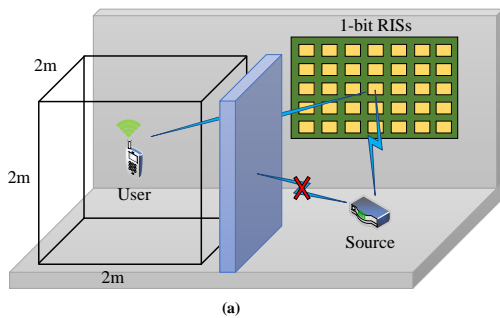


Fig. 5. (a) The simulation environment. (b) The realistic environment.

TABLE I
KEY NETWORK PARAMETERS

| Parameter | Value |
|---------------------------------------|-----------------|
| Base frequency of positional encoding | $b = 1.5$ |
| Dimension of positional encoding | $L = 20$ |
| Width of input layer | $6 \times L$ |
| Number of hidden layers | $L_h = 4$ |
| width of hidden layers | $W_h = 256$ |
| optimizer | Adam |
| Batch size | Batchsize = 256 |
| Learning rate | 10^{-3} |

TABLE II
RECEIVED SIGNAL STRENGTH OBTAINED BY DIFFERENT METHODS

| | Methods | Simulation data (dBm) | Measured data (dBm) |
|----------------|------------------|-----------------------|---------------------|
| Model-based | APX [21] | -23.93 | -29.40 |
| | SDR [22] | -23.80 | -29.27 |
| | Manopt [23] | -23.89 | -29.24 |
| Learning-based | Vanilla MLP [14] | -20.28 | -28.85 |
| | Ours | -16.85 | -26.43 |

where θ_{t+1} represents the updated parameter value, θ_t represents the current parameter value, η represents the learning rate, and $\nabla \mathcal{L}(\theta_t)$ represents the gradient of the loss function $\mathcal{L}(\theta_t)$ with respect to the parameter θ_t .

C. Performance Evaluation

1) *Comparison with Benchmarks:* The received signal strength per method is given in Table II. Each method has been experimented with in both the measured and simulated data. It is observed that the learning-based approach outperforms the model-based approach overall, and the INR-based approach proposed in this paper outperforms all four benchmarks under different data. Compared with model-based methods, the INR-based Methods demonstrate an average performance gain of approximately 7 dBm in terms of received power.

Moreover, we experimented with the performance evolution of different methods with respect to the number of training samples in the dataset. Fig. 6 shows the comparison results of accuracy between our method and vanilla MLP. As observed, in the simulation dataset, accuracy of the proposed INR-based algorithm achieves 83.58% within only 30% training data, while vanilla MLP can only achieve an accuracy of 60.89%.

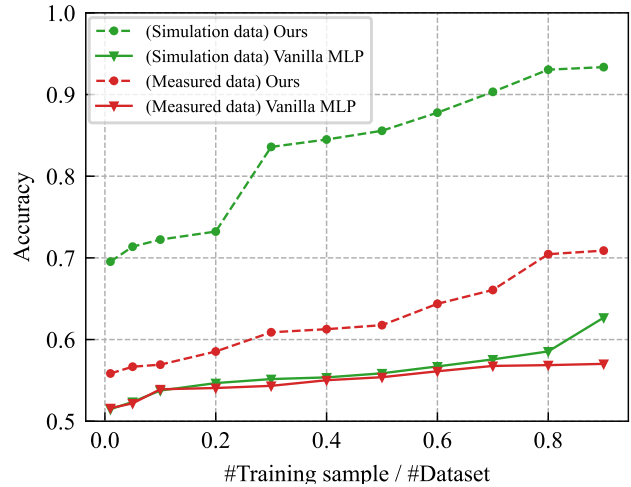


Fig. 6. The evolution of performance w.r.t the number of training samples.

As observed, in the simulation dataset, the proposed INR-based algorithm achieves an accuracy of 83.58% with only 30% of the training data, outperforming vanilla MLP, which achieves an accuracy of 60.89%. This significant performance difference can be attributed to the enhanced capability of the positional encoding in learning complex information and capturing the underlying data distribution.

2) *Ablation Studies:* We conduct ablation experiments to assess the contribution of specific components of our approach. The results are shown in Table III, where the combination of ReLU activation, positional encoding and codebook encoding outperforms alternative approaches. It is observed that positional encoding enhances the expressiveness of the network by improving the dimensionality of the input coordinates, while codebook encoding reduces the complexity of the target output space, facilitating more efficient prediction, both of which improve the performance of the neural network. Moreover, we compared the performance of various activation functions and found that ReLU consistently achieved the best results in terms of accuracy.

TABLE III
ABLATION STUDY

| Activation | PE | Simulation data | | Measured Data | |
|------------|----|-----------------|---------|---------------|---------|
| | | enc | w/o enc | enc | w/o enc |
| ReLU | ✗ | 72.88% | 55.02% | 63.67% | 56.76% |
| | ✓ | 93.04% | 90.27% | 70.45% | 62.22% |
| Sin | ✗ | 72.05% | 53.94% | 55.11% | 51.22% |
| | ✓ | 90.99% | 89.3 % | 56.27% | 52.88% |
| Tanh | ✗ | 72.71% | 58.55% | 64.29% | 56.87% |
| | ✓ | 92.32% | 88.99% | 67.12% | 60.46% |
| GELU | ✗ | 72.30% | 60.36% | 63.90% | 55.19% |
| | ✓ | 91.47% | 88.97% | 65.45% | 57.68% |
| LeakyReLU | ✗ | 73.00% | 54.79% | 66.98% | 60.47% |
| | ✓ | 92.85% | 90.74% | 67.36% | 65.65% |

V. CONCLUSION

In this paper, we investigate the codebook configuration for 1-bit RIS-aided systems. We propose a novel learning-based method using the advanced methodology of INRs. From discrete sampling, our method learns a continuous and differentiable coordinate-to-codebook representation in space. To the best of our knowledge, this is the first time INRs have been introduced to the wireless communication community, and we show its significant advantage in 1-bit RIS codebook configuration. Moreover, we propose an encoding-decoding strategy to reduce the dimension of codebooks, and improve the training efficiency and generalization of the proposed method. Experimental results on simulation and measured data demonstrate the remarkable advantages of the proposed method. Further extension of the proposed method to the scenario with multiple users, a promising future direction.

REFERENCES

- [1] Q. Wu and R. Zhang, "Towards smart and reconfigurable environment: Intelligent reflecting surface aided wireless network," *IEEE Communications Magazine*, vol. 58, no. 1, pp. 106–112, 2019.
- [2] C. Huang, G. C. Alexandropoulos, A. Zappone, M. Debbah, and C. Yuen, "Energy efficient multi-user miso communication using low resolution large intelligent surfaces," in *2018 IEEE Globecom Workshops (GC Wkshps)*. IEEE, 2018, pp. 1–6.
- [3] M. D. Renzo, M. Debbah, D.-T. Phan-Huy, A. Zappone, M.-S. Alouini, C. Yuen, V. Sciancalepore, G. C. Alexandropoulos, J. Hoydis, H. Gacanin *et al.*, "Smart radio environments empowered by reconfigurable ai meta-surfaces: An idea whose time has come," *EURASIP Journal on Wireless Communications and Networking*, vol. 2019, no. 1, pp. 1–20, 2019.
- [4] W. Tang, M. Z. Chen, X. Chen, J. Y. Dai, Y. Han, M. Di Renzo, Y. Zeng, S. Jin, Q. Cheng, and T. J. Cui, "Wireless communications with reconfigurable intelligent surface: Path loss modeling and experimental measurement," *IEEE Transactions on Wireless Communications*, vol. 20, no. 1, pp. 421–439, 2020.
- [5] X. Mu, Y. Liu, L. Guo, J. Lin, and N. Al-Dhahir, "Exploiting intelligent reflecting surfaces in noma networks: Joint beamforming optimization," *IEEE Transactions on Wireless Communications*, vol. 19, no. 10, pp. 6884–6898, 2020.
- [6] S. Yin, Y. Li, Y. Tian, and F. R. Yu, "Intelligent reflecting surface enhanced wireless communications with deep-learning-based channel prediction," *IEEE Transactions on Vehicular Technology*, vol. 71, no. 1, pp. 1049–1053, 2021.

- [7] B. Zheng, C. You, W. Mei, and R. Zhang, "A survey on channel estimation and practical passive beamforming design for intelligent reflecting surface aided wireless communications," *IEEE Communications Surveys & Tutorials*, vol. 24, no. 2, pp. 1035–1071, 2022.
- [8] Q. Wu and R. Zhang, "Beamforming optimization for wireless network aided by intelligent reflecting surface with discrete phase shifts," *IEEE Transactions on Communications*, vol. 68, no. 3, pp. 1838–1851, 2019.
- [9] M. Najafi, V. Jamali, R. Schober, and H. V. Poor, "Physics-based modeling and scalable optimization of large intelligent reflecting surfaces," *IEEE Transactions on Communications*, vol. 69, no. 4, pp. 2673–2691, 2020.
- [10] K. Feng, Q. Wang, X. Li, and C.-K. Wen, "Deep reinforcement learning based intelligent reflecting surface optimization for miso communication systems," *IEEE Wireless Communications Letters*, vol. 9, no. 5, pp. 745–749, 2020.
- [11] J. Chen, Y.-C. Liang, Y. Pei, and H. Guo, "Intelligent reflecting surface: A programmable wireless environment for physical layer security," *IEEE Access*, vol. 7, pp. 82 599–82 612, 2019.
- [12] C. Huang, A. Zappone, G. C. Alexandropoulos, M. Debbah, and C. Yuen, "Reconfigurable intelligent surfaces for energy efficiency in wireless communication," *IEEE Transactions on Wireless Communications*, vol. 18, no. 8, pp. 4157–4170, 2019.
- [13] A. Abdallah, A. Celik, A. Eltawil, and M. M. Mansour, "Multi-agent deep reinforcement learning for beam codebook design in ris-aided systems," 2022.
- [14] C. Huang, G. C. Alexandropoulos, C. Yuen, and M. Debbah, "Indoor signal focusing with deep learning designed reconfigurable intelligent surfaces," in *2019 IEEE 20th international workshop on signal processing advances in wireless communications (SPAWC)*. IEEE, 2019, pp. 1–5.
- [15] A. N. Tarekegn, M. Giacobini, and K. Michalak, "A review of methods for imbalanced multi-label classification," *Pattern Recognition*, vol. 118, p. 107965, 2021.
- [16] V. Sitzmann, J. Martel, A. Bergman, D. Lindell, and G. Wetzstein, "Implicit neural representations with periodic activation functions," *Advances in Neural Information Processing Systems*, vol. 33, pp. 7462–7473, 2020.
- [17] M. Tancik, P. Srinivasan, B. Mildenhall, S. Fridovich-Keil, N. Raghavan, U. Singhal, R. Ramamoorthi, J. Barron, and R. Ng, "Fourier features let networks learn high frequency functions in low dimensional domains," *Advances in Neural Information Processing Systems*, vol. 33, pp. 7537–7547, 2020.
- [18] H. Le, "Novel view synthesis-a neural network approach," Ph.D. dissertation, Portland State University, 2020.
- [19] R. Tucker and N. Snavely, "Single-view view synthesis with multiplane images," in *Proceedings of the IEEE/CVF Conference on Computer Vision and Pattern Recognition*, 2020, pp. 551–560.
- [20] M.-L. Zhang and Z.-H. Zhou, "A review on multi-label learning algorithms," *IEEE Transactions on Knowledge and Data Engineering*, vol. 26, no. 8, pp. 1819–1837, 2013.
- [21] Y. Zhang, K. Shen, S. Ren, X. Li, X. Chen, and Z.-Q. Luo, "Configuring intelligent reflecting surface with performance guarantees: Optimal beamforming," *IEEE Journal of Selected Topics in Signal Processing*, vol. 16, no. 5, pp. 967–979, 2022.
- [22] Q. Wu and R. Zhang, "Intelligent reflecting surface enhanced wireless network via joint active and passive beamforming," *IEEE Transactions on Wireless Communications*, vol. 18, no. 11, pp. 5394–5409, 2019.
- [23] R. Xiong, J. Zhang, X. Dong, Z. Wang, J. Liu, T. Mi, and R. C. Qiu, "RIS-aided wireless communication in real-world: Antennas design, prototyping, beam reshape and field trials," *arXiv preprint arXiv:2303.03287*, 2023.
- [24] H. Yang, X. Cao, F. Yang, J. Gao, S. Xu, M. Li, X. Chen, Y. Zhao, Y. Zheng, and S. Li, "A programmable metasurface with dynamic polarization, scattering and focusing control," *Scientific Reports*, vol. 6, no. 1, pp. 1–11, 2016.
- [25] H. Yang, F. Yang, S. Xu, Y. Mao, M. Li, X. Cao, and J. Gao, "A 1-bit 10 × 10 reconfigurable reflectarray antenna: design, optimization, and experiment," *IEEE Transactions on Antennas and Propagation*, vol. 64, no. 6, pp. 2246–2254, 2016.